

Electronic Supplementary Information (ESI) for:

Simulated photoelectron intensities at the aqueous solution–air interface for flat and cylindrical (microjet) geometries

Giorgia Olivieri,^a Krista M. Parry,^b Cedric J. Powell,^c Douglas J. Tobias,^b and Matthew A. Brown^{a*}

^aLaboratory for Surface Science and Technology, Department of Materials, ETH Zürich, Switzerland.

^bDepartment of Chemistry, University of California, Irvine, California, USA.

^cMaterials Measurement Science Division, National Institute of Standards and Technology, Gaithersburg, Maryland, USA.

E-mail: matthew.brown@mat.ethz.ch

Table ESI-1. Information depths ($P = 95\%$, $\alpha = 0^\circ$) for semi-infinite bulk solutions of pure water and homogeneous 1 mol/L NaI calculated using SESSA with linear polarized light. Information depths extrapolated from a linear fit of the calculated values are marked with an asterisk.

Kinetic Energy (eV)	S (nm)	S (nm)
	H ₂ O	1 mol/L NaI
65	1.47	1.40
100*	1.97	1.89
150*	2.37	2.27
200	2.71	2.60
250*	3.17	3.04
300*	3.57	3.42
350*	3.97	3.80
400*	4.37	4.18
450*	4.78	4.57
500	5.36	5.13
550*	5.58	5.33
600*	5.98	5.71
650*	6.38	6.09
700*	6.78	6.48
750*	7.18	6.86
800	7.88	7.53
850*	7.98	7.62
900*	8.38	8.01
950*	8.78	8.39
1000	9.22	8.81
1050*	9.58	9.15
1100*	9.98	9.53
1150*	10.38	9.92
1200*	10.78	10.30
1250	11.12	10.63
1300*	11.58	11.06
1350*	11.98	11.45
1400*	12.38	11.83
1450*	12.78	12.21
1500	13.00	12.41

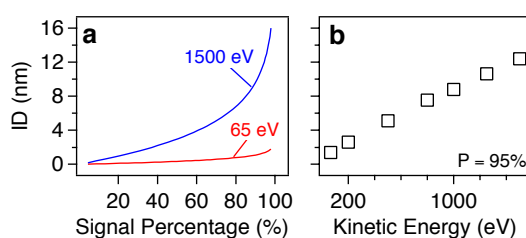


Fig. ESI-1. (a) Information depth (ID) at 65 eV and 1500 eV of a semi-infinite solution of 1 mol/L NaI as a function of the percentage of the detected signal when using linear polarized light and $\alpha = 0^\circ$. (b) IDs of liquid water for $P=95\%$ as a function of photoelectron kinetic energy when $\alpha = 0^\circ$.

Methods

Simulation of Electron Spectra for Surface Analysis (SESSA). XPS signal intensities are simulated using the SESSA software package developed by Werner *et al.*¹ SESSA is a NIST standard reference database² that contains all data needed for quantitative simulations of XPS and Auger-electron spectra. Data retrieval is based on an expert system that queries the databases for each needed parameter. SESSA provides the spectral shape of each photoelectron peak using a model of signal generation in XPS that includes multiple inelastic and elastic scattering of the photoelectrons. In order to minimize the computation time, an efficient Monte Carlo code is employed based on the trajectory-reversal method. In contrast to

conventional Monte Carlo codes where electrons are tracked based on their trajectories from the source to the detector, the trajectory-reversal approach tracks electrons in the opposite direction, starting from the detector and working back to the point of origin. Thus, all electrons contribute to the signal, which results in significantly decreased simulation times.

For the SESSA simulations reported in this Communication, the orientation of the analyzer axis is perpendicular to the X-ray source, while the sample surface normal orientation is varied from 0° (parallel to the analyzer axis) to 90° (perpendicular to the analyzer axis). The excitation source is a 100% linearly polarized X-ray beam. The polarization vector is rotated 54.7° from the analyzer detection axis, which corresponds to the so-called magic angle in which the XPS intensity is independent of the emission angle. Since we are simulating synchrotron-based experiments in which X-rays are focused in a relatively small area, the illuminated area on the sample is independent of the emission angle.

Other details of our SESSA simulations have been discussed previously.³A convergence factor of 10^{-6} has been used for all simulations and the Mott approximation has been used to take into account elastic-scattering effects. The total density for pure water and bulk 1 mol/L NaI has been set to 9.90×10^{22} atoms/cm³ and 9.42×10^{22} atoms/cm³, respectively, while the band gap is assumed 7.9 eV for both solutions. Our calculations employ electron IMFPs calculated via the semi-empirical TPP-2M formula of Tanuma *et al.*⁴ integrated within SESSA. The calculated IMFPs, which depend on the material density, atomic or molecular mass, number of valence electrons per atom or molecule, and the band gap energy, are expected to have uncertainties of about 10%, although the uncertainty could be larger for a small number of materials. For the Na/I ion intensity ratios a total of 13 photoelectron energies were simulated and the simulated intensities were normalized by the atomic photoionization cross sections of Yeh and Lindau⁵ integrated within SESSA.

Molecular Dynamics (MD) Simulations. Molecular dynamics simulations of the 1 mol/L NaI solution were performed using the GROMACS simulation suite⁶. 1728 water molecules and 32 NaI ion pairs were placed in a 3.0 nm x 3.0 nm x 14.0 nm unit cell in the slab geometry. Periodic boundary conditions were implemented in all three dimensions. The simulation was carried out for 100 μs using a timestep of 2 fs. The temperature was held at 300 K using a Berendsen thermostat with an additional stochastic term that ensures the correct kinetic energy distribution.⁷ Water molecules were modeled using the Simple Point Charge/Extended (SPC/E) force field,⁸ and the Lennard-Jones parameters for the ions were parameterized by Netz and coworkers.⁹ Electrostatic interactions were calculated using the Particle-Mesh Ewald method,¹⁰ and a cutoff of 0.9 nm was used for the Lennard-Jones interactions and the real-space part of the Ewald sum. Water molecules were held rigid using the SETTLE algorithm.¹¹ Atom density profiles were computed with respect to the instantaneous interface as described previously.^{3, 12} The average bulk concentration calculated from the composition of the innermost 2 nm of the slab was 0.96 mol/L.

Liquid jet properties. Not all readers are familiar with the liquid jets used for XPS experiments. Here we provide a few key details that might help to better understand the simulation results of the main manuscript. Liquid jets are generated by forcing the liquid under investigation through thin quartz capillaries of inner diameter ~6–30 μm using a standard commercial high-pressure liquid chromatography (HPLC) pump. These liquid jets are free flowing inside the vacuum chamber and provide a continuously refreshed interface. The liquid jet is spatially overlapped with synchrotron radiation and XPS is performed. The typically size of the X-ray beam (fwhm) is on the order of 10's of μm.

Calculation of the information depth (ID)

The IDs of Table ESI-1 are calculated for semi-infinite solutions using SESSA. For this purpose the sample has been sliced into layers and the photoelectron intensity of the O 1s has been simulated for each layer separately for a given photoelectron kinetic energy. By doing this operation the total photoelectron signal is obtained as a function of depth and it is then easy to convert it into an ID as a function of the signal percentage. The number of slices as well as the slices' thickness varied with the kinetic energy of the photoelectron in order to adjust the total sample thickness to the ID for that particular energy. All the simulations have been performed with linearly polarized light at the so-called magic angle. The analyser polar acceptance angle is 1° and the average emission angle of the photoelectrons is 0°.

Average emission angle of a cylindrical microjet of pure water

In order to calculate the limit in Eq. 2 of the main text we have simulated the O 1s intensity for a microjet of pure water using SESSA for 91 surface tilt angles between 0° and 90° in increments of 1°. The average emission angle is calculated (see Fig. ESI-2) using planes with separation of 1°, 2°, 5° or 10°, which corresponds to using 91, 46, 19 and 10 planes, respectively. As the number of planes tends to infinity the surface tilt angle increments tend to zero. For this reason, an extrapolation of the average emission angle to zero surface tilt angle step is necessary to find the correct average emission angle. The results of Fig. ESI-2 show a linear extrapolation.

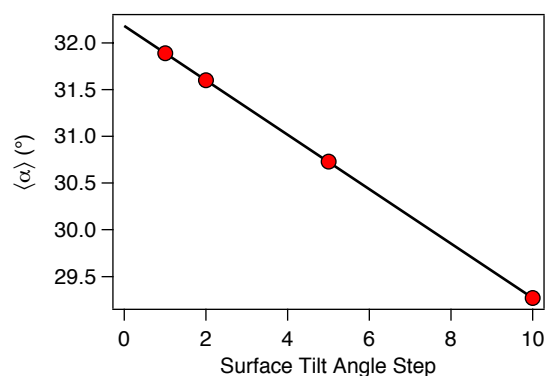


Fig. ESI-2. Average emission angle as a function of the surface tilt angle increment. A linear extrapolation to $x = 0$ yields the average emission angle used in the main text.

Comparison of the average emission angle of a cylindrical microjet of pure water with that of a homogeneous solution of 1 mol/L NaI

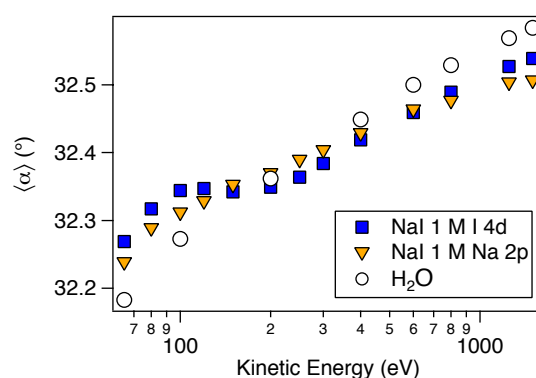


Fig. ESI-3. Average emission angle for a cylindrical microjet of pure water (open black markers) and for a homogeneous solution of 1 mol/L NaI.

I 4d/ Na 2p ratio for a homogeneous solution of 1 mol/L NaI as a function of kinetic energy

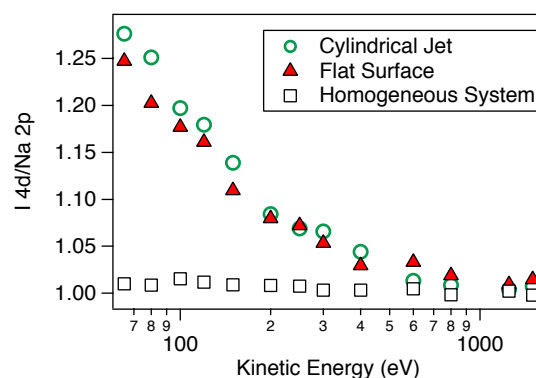


Fig. ESI-4. (open black squares) I 4d/Na 2p ion ratios calculated from SESSA simulation for a semi-infinite bulk homogeneous solution of 1 mol/L NaI. These results verify that the cross-sections used to normalize the simulated photoelectron intensities result in stoichiometric ion intensity ratios for all kinetic energies. Results for the complete molecular dynamics interface are included for comparison (these data are plotted in Fig. 4 of the main text).

References

1. W. Smekal, W. S. M. Werner and C. J. Powell, *Surf Interface Anal*, 2005, **37**, 1059-1067.
2. W. S. M. Werner, W. Smekal and C. J. Powell, *NIST Database for the Simulation of Electron Spectra for Surface Analysis, Version 2.0, Standard Reference Data program Database 100*, Department of Commerce, National Institute of Standards and Technology, Gaithersburg, Maryland, 2014.
3. G. Olivieri, K. M. Parry, C. J. Powell, D. J. Tobias and M. A. Brown, *J Chem Phys*, 2016, **144**.
4. S. Tanuma, C. J. Powell and D. R. Penn, *Surf Interface Anal*, 1994, **21**, 165-176.
5. J. J. Yeh and I. Lindau, *Atom Data Nucl Data*, 1985, **32**, 1-155.
6. B. Hess, C. Kutzner, D. van der Spoel and E. Lindahl, *J Chem Theory Comput*, 2008, **4**, 435-447.
7. G. Bussi, D. Donadio and M. Parrinello, *J Chem Phys*, 2007, **126**.
8. H. J. Berendsen, J. R. Grigera and T. P. Straatsma, *J Phys Chem-Us*, 1987, **91**, 6269-6271.
9. D. Horinek, A. Herz, L. Vrbka, F. Sedlmeier, S. I. Mamatkulov and R. R. Netz, *Chem Phys Lett*, 2009, **479**, 173-183.
10. U. Essmann, L. Perera, M. L. Berkowitz, T. Darden, H. Lee and L. G. Pedersen, *J Chem Phys*, 1995, **103**, 8577-8593.
11. S. Miyamoto and P. A. Kollman, *J Comput Chem*, 1992, **13**, 952-962.
12. A. P. Willard and D. Chandler, *J Phys Chem B*, 2010, **114**, 1954-1958.